Coronary artery analysis: Computer-assisted selection of best-quality segments in multiple-phase coronary CT angiography

Chuan Zhou,[a] Heang-Ping Chan, Lubomir M. Hadjiiski, Aamer Chughtai, Jun Wei, and Ella A. Kazerooni
Department of Radiology, The University of Michigan, Ann Arbor, Michigan 48109-0904

(Received 1 February 2016; revised 8 June 2016; accepted for publication 13 August 2016; published 6 September 2016; corrected 27 September 2016)

Purpose: The authors are developing an automated method to identify the best-quality coronary arterial segment from multiple-phase coronary CT angiography (cCTA) acquisitions, which may be used by either interpreting physicians or computer-aided detection systems to optimally and efficiently utilize the diagnostic information available in multiple-phase cCTA for the detection of coronary artery disease.
Methods: After initialization with a manually identified seed point, each coronary artery tree is automatically extracted from multiple cCTA phases using our multiscale coronary artery response enhancement and 3D rolling balloon region growing vessel segmentation and tracking method. The coronary artery trees from multiple phases are then aligned by a global registration using an affine transformation with quadratic terms and nonlinear simplex optimization, followed by a local registration using a cubic B-spline method with fast localized optimization. The corresponding coronary arteries among the available phases are identified using a recursive coronary segment matching method. Each of the identified vessel segments is transformed by the curved planar reformation (CPR) method. Four features are extracted from each corresponding segment as quality indicators in the original computed tomography volume and the straightened CPR volume, and each quality indicator is used as a voting classifier for the arterial segment. A weighted voting ensemble (WVE) classifier is designed to combine the votes of the four voting classifiers for each corresponding segment. The segment with the highest WVE vote is then selected as the best-quality segment. In this study, the training and test sets consisted of 6 and 20 cCTA cases, respectively, each with 6 phases, containing a total of 156 cCTA volumes and 312 coronary artery trees. An observer preference study was also conducted with one expert cardiothoracic radiologist and four nonradiologist readers to visually rank vessel segment quality. The performance of our automated method was evaluated by comparing the automatically identified best-quality segments identified by the computer to those selected by the observers.
Results: For the 20 test cases, 254 groups of corresponding vessel segments were identified after multiple phase registration and recursive matching. The AI-BQ segments agreed with the radiologist's top 2 ranked segments in 78.3% of the 254 groups (Cohen's kappa 0.60), and with the 4 nonradiologist observers in 76.8%, 84.3%, 83.9%, and 85.8% of the 254 groups. In addition, 89.4% of the AI-BQ segments agreed with at least two observers' top 2 rankings, and 96.5% agreed with at least one observer's top 2 rankings. In comparison, agreement between the four observers' top ranked segment and the radiologist's top 2 ranked segments were 79.9%, 80.7%, 82.3%, and 76.8%, respectively, with kappa values ranging from 0.56 to 0.68.
Conclusions: The performance of our automated method for selecting the best-quality coronary segments from a multiple-phase cCTA acquisition was comparable to the selection made by human observers. This study demonstrates the potential usefulness of the automated method in clinical practice, enabling interpreting physicians to fully utilize the best available information in cCTA for diagnosis of coronary disease, without requiring manual search through the multiple phases and minimizing the variability in image phase selection for evaluation of coronary artery segments across the diversity of human readers with variations in expertise. [http://dx.doi.org/10.1118/1.4961740]

Key words: coronary CT angiography, image analysis, computer-aided reading

1. INTRODUCTION

Coronary artery disease (CAD) is the most common type of heart disease and the leading cause of death worldwide.[1] Of the over 16×10^6 Americans with CAD, 445 000 die of this annually, including 151 000 from acute myocardial infarction (MI).[2] When the coronary arteries are narrowed or blocked by the accumulation of atherosclerotic plaque, the reduction of oxygen-rich blood flow to the heart muscle can cause angina or MI. Imaging CAD is a demanding task that requires both high

spatial resolution due to the small size of the coronary arteries, and high temporal resolution to reduce motion artifacts from the beating heart. With the rapid advancement of computed tomography (CT) techniques, electrocardiographic (ECG)-gated coronary CT angiography (cCTA) with multidetector rows is a promising modality for not only detecting CAD but also for quantifying and characterizing plaque.[3–7] With the cyclic and rhythmic motion of the heart, different parts of the heart and therefore different parts of the coronary arteries move at different phases in a cardiac cycle. For example, the right-sided coronary arteries are generally better seen at end-systole, while the left-sided coronary arteries are generally better seen at end-diastole.[7] ECG-gating enables data acquisition at a specific phase or phases of the cardiac cycle over a series of cycles so that the cCTA examination with data reconstructed at multiple phases. This increases the probability that good quality images of the coronary arteries can be found on at least one of the phases.

Multiple-phase cCTA allows the interpreting physicians to search for the best-quality phase for each artery segment during interpretation to achieve optimal diagnostic accuracy. The search for the best-quality images for each individual artery segments is time consuming and may vary across readers of varying expertise and experience. In clinical practice, the radiologists may only use very few phases to interpret all coronary artery segments because of their workload. Some segments may therefore be interpreted in a suboptimal phase and the other available phases are under-utilized. Automatic selection of the best-quality segment among the corresponding segments in the multiple-phase cCTA for each coronary artery should be useful as a preprocessing step for both the interpreting physician and also for a computer-aided detection system.[8]

Automated determination of a single "optimal" cardiac phase, or the phase of minimal cardiac motion, among the available multiple phases has been reported in a number of studies.[9–14] According to the 17-segment model defined by American Heart Association (AHA), for each cCTA scan, 17 major coronary arterial segments are considered clinically significant.[15] However, the selection of only one best phase cannot provide the optimal image quality for detection of atherosclerotic plaques in each individual coronary artery segment because it is unlikely that all coronary arteries have the best quality in the same phase. We are developing an automated selection method to select the best quality segment among all phases for each individual coronary artery segment. The resulting collection of artery segments may be considered a "virtual" composite coronary arterial tree, of which each individual segment may come from a different phase among the available multiple phase cCTA examination. The composite arterial tree can be prepared ahead of the interpreting physician's use or as a preprocessing step in computer-aided analysis. Our previous pilot study[16] demonstrated the feasibility of the automated selection method using a single feature and two cCTA cases. In the current study, we further improved the matching of corresponding segments from different phases, extracted new features from the straightened curved planar reformation (CPR) vessel volume and the original CT volume, and designed a weighted voting ensemble (WVE) classifier for identification of the best-quality segments. The performance of our automated method for identification of the best-quality coronary segments was evaluated by comparison with manual selection in an observer preference study using a test set.

2. MATERIALS AND METHODS

2.A. Data sets

A data set containing 26 ECG-gated cCTA cases retrospectively collected from patient files at the University of Michigan Hospital with Institutional Review Boards (IRB) approval was used. The cCTA cases were acquired with GE multidetector CT scanners (GE Healthcare, Milwaukee, WI), 120–140 kVp, 300–600 mAs, and reconstructed at 0.625 mm slice interval with 0.488 mm in-plane pixel size. Six reconstructed ECG-gated phases were available for all 26 cases, resulting in a total of 156 cCTA volumes and a total of 312 left and right coronary artery trees combined. The data set was randomly divided by case into training and test sets with 6 and 20 cases, respectively.

2.B. Methods

Figure 1 shows the schematic diagram of our automated approach to the identification of best-quality coronary artery segments from a multiple-phase cCTA examination. The processes on the left blocks were developed previously; the current study focused on the development of the methods on the right blocks. The coronary arteries are enhanced using our multiscale coronary artery response (MSCAR) method, and the left and right coronary artery trees are extracted from the volume of each cCTA phase using a 3D rolling balloon region growing (RBG) method.[17,18] An automated registration method is then used to align the multiple-phase artery trees.[19] The corresponding coronary artery segments are identified among the registered arterial trees and each segment is straightened by the CPR method.[8,20] Several features are extracted from each vessel segment as quality indicators in the original CT volume and the straightened CPR volume. A newly designed WVE classifier is finally used to select the best-quality coronary segment among the corresponding segments. Because there is no gold standard to determine the best-quality vessels, we evaluated the performance of our automated method by comparing the best-quality coronary segments obtained by automated selection from multiple phases to those by manual selection in an observer preference study. The agreement between observers was also evaluated using Cohen's kappa statistics (using *R*, a free software supported by the *R* foundation for statistical computing) as a reference for the variability of subjective selection.[21]

2.B.1. Coronary arterial tree extraction

We have previously developed an MSCAR-RBG method for extraction of coronary arterial trees.[17,18] Briefly, the heart region is first extracted by an adaptive thresholding

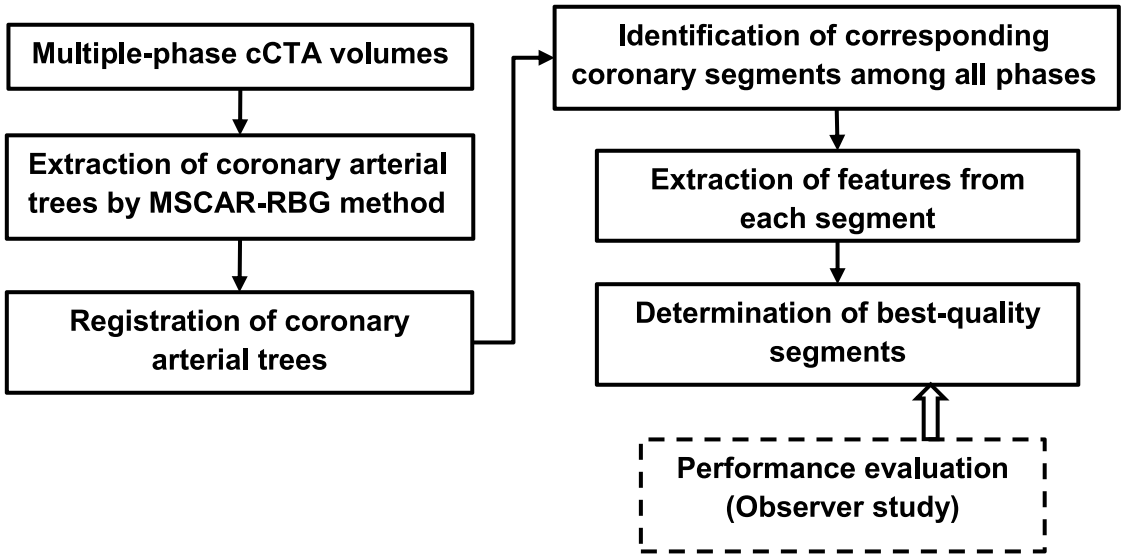

FIG. 1. Schematic diagram of our method for identification of the best-quality coronary artery segments from multiple-phase cCTA. Multiscale coronary artery response enhancement and 3D rolling balloon region growing (MSCAR-RBG) vessel segmentation and tracking method (Refs. 17 and 18).

method based on expectation–maximization estimation and a morphological operation. The vascular structures within the heart region are enhanced based on the analysis of a multiscale coronary artery response function specifically designed to extract information from the eigenvalues of Hessian matrices for enhancing coronary vascular structures.[22] The MSCAR-enhanced left and right coronary artery trees are then segmented and tracked by the RBG method. At present, the RBG method is initialized by two manually identified seed points located at the origins of the left and right coronary arteries for each phase. After initialization, all subsequent processes are automated. In the RBG method, a rolling balloon adaptively adjusts its diameter according to the local vessel size and finds the branches and the next tracking point; region growing is then used to identify the connected voxels along the tracked vessel. The RBG method thus determines the centerlines, the branching points, and the artery segments in each tracked coronary tree.

2.B.2. Identification of corresponding coronary segments in different phases

We have previously designed an automated registration method to co-register the multiple-phase left or right coronary arterial trees extracted from the cCTA volumes.[19] Briefly, the left and right coronary trees extracted from the adjacent phase pairs (e.g., phases of 70% and 75%, 75% and 80%), where the displacements of the arteries in the adjacent phases are relatively small, are first registered based on a cubic B-spline method with fast localized optimization (CBSO). The group of registered trees from the adjacent phases (e.g., 40%, 45%, and 50%) is then further registered with that from the farther phases (e.g., 70%, 75%, and 80%). For the latter registration of two groups that potentially have large displacements, a global registration based on an affine transformation with quadratic terms and nonlinear simplex optimization (AQSO) is employed first to reduce the displacements, followed by a local registration using CBSO to refine the AQSO registered volumes. The details of our registration method were described elsewhere.[19]

After the registration, for a segment S_i in phase i, to find its corresponding segment S_j in phase j, where $j \neq i$, the shortest distance of the t-th center point C_j^t on segment S_j to the segment S_i is calculated by Euclidean distance d as

$$D\left(C_j^t, S_i\right) = \min\left\{d\left(C_j^t, C_i^u\right) : C_i^u \in c\right\}, \tag{1}$$

where C_i^u is the u-th center point in the set of center points c along the segment S_i. The segment S_j in phase j is determined as a candidate of corresponding segments for S_i by the criterion that greater than a threshold percentage P of its center points are within a distance of $D_{\max}$ to the center points of the segment S_i. K ($K \geq 0$) candidate segments for S_i can be identified from each phase j. Among the candidate segments S_j^k ($k = 1, \ldots, K$) from phase j, the corresponding segment S_j' is then determined as the one that has the maximum number of center points satisfying the above criterion,

$$S_j' = \underset{k}{\operatorname{argmax}} N(S_j^k), \tag{2}$$

where $N\left(S_j^k\right)$ is the number of center points along the k-th candidate S_j^k of the corresponding segments that satisfy the above criterion defined by P and $D_{\max}$. P and $D_{\max}$ were experimentally determined to be 70% and 2 mm, respectively, using the training set.

We designed a recursive coronary segment matching (RCSM) method to identify the corresponding segments in different cCTA phases as follows. The longest segment is first selected from all phases by counting the maximum number of center points along the branches from the seed point located at the origins of the left or right coronary arteries to the end points of the artery trees. The corresponding segments in the other phases are then identified by Eqs. (1) and (2). The above procedure is recursively repeated by selecting the longest segment from the remaining unmatched segments in the multiple-phase

coronary trees, and finding its corresponding segments in the other phases, until no unmatched segments are left in all phases. Short segments (<20 mm) are discarded. The process is performed separately in the left and right coronary trees. For a cCTA exam with six phases, each group of corresponding arteries could contain up to six segments, one from each phase. Some groups might have less than six segments if the vessels are blurred or poor quality and could not be tracked in one or more phases. Note that, in our method, an artery segment determined in the first iteration of RCSM starts from the seed point at the origin of one of the coronary trees to the farthest point that the MSCAR-RBG algorithm can track along the tree. The next longest artery segment will be searched from the remaining unmatched tree branches, excluding an entire vessel or the portions of a vessel already used in the previous matches. Therefore, the other artery segments in the subsequent iterations start from the bifurcations where the artery branches off from an already matched segment in the previous iterations. For simplicity, we use the term "artery segment" to denote the portions of the artery found and matched in each iteration but it can be different from those defined in the 17-segment model of the AHA.[15]

2.B.3. Determination of the best-quality segments

The corresponding artery segments in the different phases are first straightened using a CPR method.[8,20,23] The CPR method resamples the cCTA volume in planar cross sections perpendicular to the tracked centerline, and reformats the original curved vessel and its neighboring region into a straightened volume.

In a straightened CPR volume for a vessel segment, the gray level of the cross section of the cylinderlike vessel volume is gradually decreasing from the vessel center to the vessel wall. For a good quality vessel with less artifacts caused by cardiac motion, contrast timing, CT reconstruction noises, etc., the contrast filling in the vessel lumen is relatively uniform so that the radial gradient vectors approximately point to the centerline with the maximum radial gradients occurring at the vessel wall, while the gradient vectors along the vessel approximately point parallel to the centerline. Based on the above assumptions, for each segment in each phase, we designed the following four features extracted from the original CT volume and the straightened CPR volume as quality indicators.

2.B.3.a. (f_1) *Mean radial gradient of vessel wall (mRGV).* A measure of vessel sharpness, referred to as mRGV, is defined as the mean radial gradients of voxels located at or adjacent to the vessel wall. On a vessel cross sectional plane perpendicular to the centerline and centered at a center point C^t ($t = 1, \ldots, N_c$, where N_c is the number of center points in the vessel segment), the radial gradient g_m at the m-th voxel along a radius from the vessel center to the vessel wall on the cross sectional plane is calculated as

$$g_m = \frac{1}{3}\left(\sum_{i=1}^{3} I_{m-i} - \sum_{i=1}^{3} I_{m+i}\right), \tag{3}$$

where I_{m-i} and I_{m+i} are the CT values of the voxels before and after the m-th voxel along the radius, where $m = 4, 5, \ldots N_r - 3$, and N_r is the number of voxels along the radius from the vessel center to the edge of the reformatted cross sectional plane in the CPR volume of the vessel. The radial gradient of the lumen at center point C^t is then calculated as the average of the maximum gradients along all radii,

$$g_t = \frac{1}{360}\sum_{\theta=1^\circ}^{360^\circ} \max\left(g_m^\theta\right), \tag{4}$$

where g_m^θ is the gradient g_m along the radius at angle θ (with respect to the horizontal direction x-axis in the CPR volume). Finally, mRGV is calculated as the mean of the g_t over all center point C^t along the vessel segment,

$$\text{mRGV} = \frac{1}{N_c}\sum_{t=1}^{N_c} g_t. \tag{5}$$

2.B.3.b. (f_2) *Vessel smoothness measure (VSM).* A vessel smoothness measure (VSM) is calculated as the mean of the gradients within the lumen in the direction parallel to the centerline where the gradients are calculated similar to Eq. (3), but with the gradient direction pointing parallel to the centerline,

$$\text{VSM} = \frac{1}{N_v}\sum_{m=1}^{N_v} g_m, \tag{6}$$

where N_v is the number of voxels of the extracted coronary segment in the CPR volume.

2.B.3.c. (f_3) *Vessel blurriness measure (VBM).* The CT values accumulated along the direction parallel to the vessel centerline within the vessel lumen in the CPR volume are calculated as

$$A(x,y) = \frac{1}{N_c}\sum_{z=1}^{N_c} I(x,y,z), \tag{7}$$

where x, y, and z are the voxel coordinates of the CRP volume. (x, y) are the coordinates on the cross sectional plane and z is the direction parallel to the centerline. $A(x,y)$ is therefore a 2D distribution of the CT values averaged over all cross sectional planes of the vessel. A 2D Gaussian function is then fitted to $A(x,y)$. VBM is defined as the mean of the standard deviations σ_x and σ_y of the fitted 2D Gaussian function,

$$\text{VBM} = \frac{1}{2}\left(\sigma_x + \sigma_y\right). \tag{8}$$

2.B.3.d. (f_4) *Ratio of mean CT value in the vessel central regions relative to that in the surrounding region within the lumen (mRCS).* Within the vessel lumen in the original CT volume, the ratio of the mean CT value in a small cube to the mean CT value in a large cube enclosing but excluding the voxels of the small cube is defined as

$$\text{RCS}\left(C^t\right) = \frac{\mu_C}{\mu_S}, \tag{9}$$

where μ_C is the mean CT value in a $3\times3\times3$ cube, and μ_S is the mean CT value in a $7\times7\times7$ cube excluding the voxels in the central $3\times3\times3$ cube; both cubes are centered at the center

point C^t. The mRCS is then calculated as the mean of the RCS values over all center points along the vessel segment,

$$\mathrm{mRCS} = \frac{1}{N_c}\sum_{t=1}^{N_c}\mathrm{RCS}(C^t). \tag{10}$$

For each corresponding vessel segment identified from the different phases by the RCSM method, the above four features are extracted as quality indicators. Each quality indicator is used as a voting classifier to cast vote for the corresponding vessel segment. The vote of the segment S_j in phase j by quality indicator f_i ($i = 1, 2, 3, 4$) is defined as

$$v(f_i,S_j) = \begin{cases} V_1 & \text{if } f_i(S_j) > \mu(f_i) \\ V_2 & \text{else} \end{cases}, \tag{11}$$

where $f_i(S_j)$ is the quality indicator f_i measured in the segment S_j, and $\mu(f_i)$ is the mean of f_i over the corresponding segments identified by RCSM method (e.g., six segments from six phases). For the four features defined above, the larger the values of f_1 and f_4, and the smaller the values of f_2 and f_3 indicate better vessel quality. Therefore, $V_1 = 1$ indicates better quality for f_1 and f_4, $V_2 = 1$ indicate better quality for f_2 and f_3, and Eq. (11) can be rewritten as

$$v(f_i,S_j) = \begin{cases} 1 & \text{if } f_i(S_j) > \mu(f_i) \\ 0 & \text{else} \end{cases} \quad \text{for } i = 1,4, \tag{12}$$

$$v(f_i,S_j) = \begin{cases} 1 & \text{if } f_i(S_j) < \mu(f_i) \\ 0 & \text{else} \end{cases} \quad \text{for } i = 2,3. \tag{13}$$

We designed a new WVE classifier to combine the votes of the four voting classifiers for each corresponding segment S_j,

$$\mathrm{WVE}(S_j) = w_1 v(f_1,S_j) + w_2 v(f_2,S_j) + w_3 v(f_3,S_j) + w_4 v(f_4,S_j), \tag{14}$$

where w_1, w_2, w_3, and w_4 are the ensemble weights of the four voting classifiers and are determined by a linear discriminant analysis using the training set. The segment with the highest WVE score is determined to be the best-quality coronary segment among the corresponding segments from the available phases.

For the training set of 6 cCTA cases, our methods extracted, tracked, and registered 324 segments for the left and right coronary artery trees, which were then matched into 72 groups by RCSM. The best-quality coronary artery segments were visually identified by an experienced radiologist and used as reference standard for the training of the WVE classifier.

2.B.4. Observer preference study

Because there is no ground truth to measure which coronary segment has the best quality among the corresponding segments in different phases, we designed an observer preference study to evaluate whether the best quality of the coronary vessels selected by our automated method agreed with the selection by human observers (Fig. 2). We developed a computer graphical user interface (GUI) for the observer study. An example of a displayed vessel segment to the observer is shown in Fig. 3. The CPR images of the corresponding coronary segments in six phases identified by our RCSM method were displayed side by side on a Siemens DSB 2003D, 3-mega-pixel (1536×2048) 20.8 in. gray scale LCD monitor. Note that the six phases of the corresponding vessel segments were displayed in a randomized order for each segment and each observer, rather than in consecutive phases (e.g., 40%, 45%, 50%, 70%, 75%, and 80%), to avoid bias in the observer's selection because some cardiac phases are expected to have less motion artifacts clinically. Each observer was blinded to the quality indicators and visually ranked the quality of the vessel segments from 1 to 6 (1 is the best) by clicking the checkbox on the right side of each segment image. The GUI provided functions that allowed the observer to adjust the window settings and zoom to improve visualization as needed.

2.B.5. Performance evaluation

One experienced cardiothoracic radiologist and four experienced medical imaging researchers participated in this study as observers. From the 20 test cCTA cases, 999 segments were extracted, tracked, and registered for the left and right coronary artery trees. The RCSM method matched

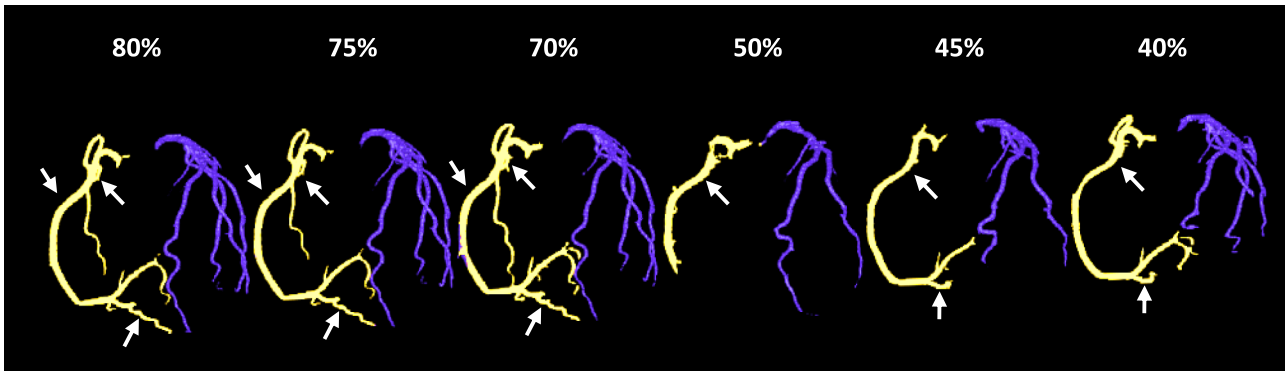

FIG. 2. An example of the segmented left (blue) and right (yellow) coronary artery trees in cCTA scans acquired with ECG gating and reconstructed at six phases (80%, 75%, 70%, 50%, 45%, and 40%) using the MSCAR-RBG method. One group of the corresponding artery segments that were identified in the six phases for a tracked vessel are pointed out by white arrows. (See color online version.)

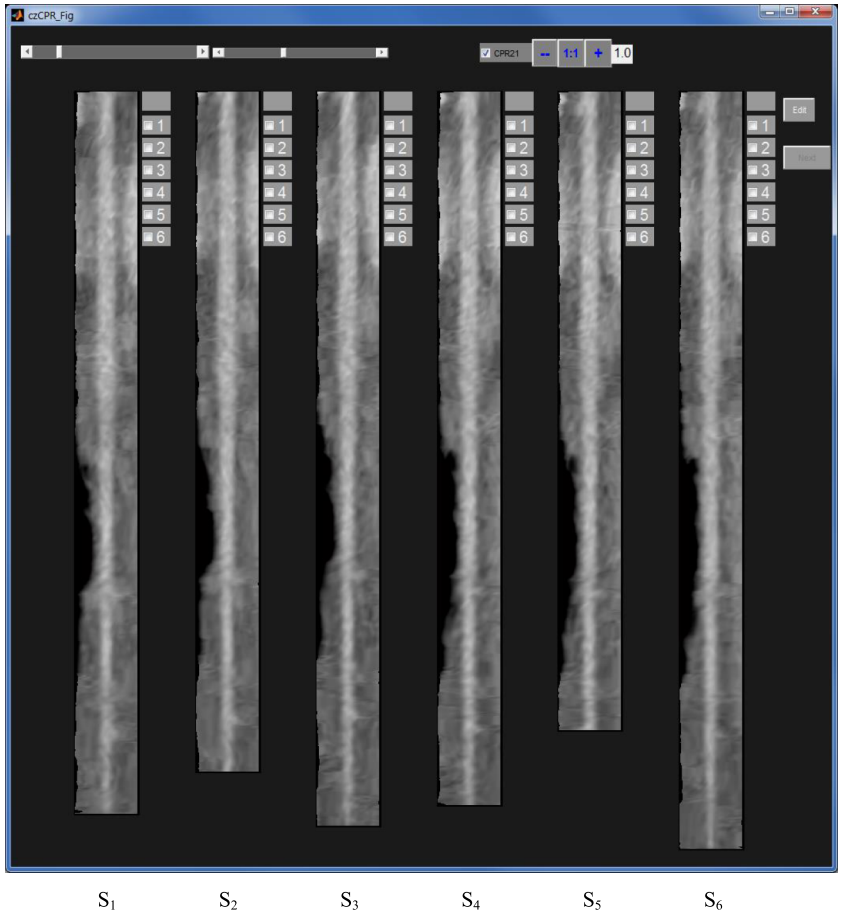

FIG. 3. A screen shot of our in-house developed graphic user interface for the observer preference study. The CPR images of corresponding coronary segments in six phases determined by our RCSM method were displayed side by side in a randomized order for each segment and each observer. The rankings of the vessel quality ranged from 1 to 6 with 1 being the best. The labels S_j ($j = 1, \ldots, 6$) are added to indicate the order of the images in the figure to facilitate the discussion in Table III; they were not displayed during the observer experiment.

the corresponding vessel segments from the multiple phases into 254 groups, which were displayed and visually rated by each observer in the preference study. Some groups did not have corresponding segments from all six phases because vessel segmentation and tracking might fail in phases that had poor quality due to motion, poor contrast filling, and/or noise. Figure 4 shows an example that had only five corresponding segments as determined by the RCSM method. The performance of the automated identification of the best-quality artery segments was evaluated as the percentages of the 254 groups for which the automatically identified best-quality (AI-BQ) segments agreed with the observers' top ranked segments, i.e., the observers' preferred artery segments, among the available phases.

3. RESULTS

Table I shows the agreement between the automated method and human observers in identifying the best-quality coronary artery segments from multiple-phase cCTA for the test set. If the AI-BQ segment being within the observer's top 2 rankings is considered to be in agreement, the agreement between AI-BQ and the radiologist is 78.3%, and between AI-BQ and the other four observers are 76.8%, 84.3%, 83.9%, and 85.8%, respectively. If the AI-BQ segment being within the observer's top 3 rankings is considered to be in agreement, the results are 89.8%, 87.8%, 92.9%, 89.4%, and 94.5%, respectively. Among the five observers, 96.5% of the AI-BQ segments agree with at least one observer's top 2 rankings, and 89.4% of AI-BQ segments agree with at least two observers' top 2 rankings. Table II shows the agreement between the radiologist and the other four observers. The percentages of the 254 groups for which an observer's top ranked segment agreed with the radiologist's top 2 ranked segments ranged from 76.8% to 82.3% and the Cohen's kappa statistics ranged from 0.56 to 0.68. Three of the four observers show substantial agreement with the radiologist and one has moderate agreement. In comparison, the agreement between the AI-BQ segment and the radiologist's top 2 rankings has a kappa value of 0.60 ± 0.05, which is at the borderline between moderate and substantial agreement.

Figure 5 shows the distributions of the percentages of AI-BQ segments and the segments within the five observers' top 2 rankings in the six cCTA phases for the left and right coronary trees. The percentages for the AI-BQ segments in the left and right coronary trees were calculated relative to the total number of vessel segment groups in each tree, 147 and

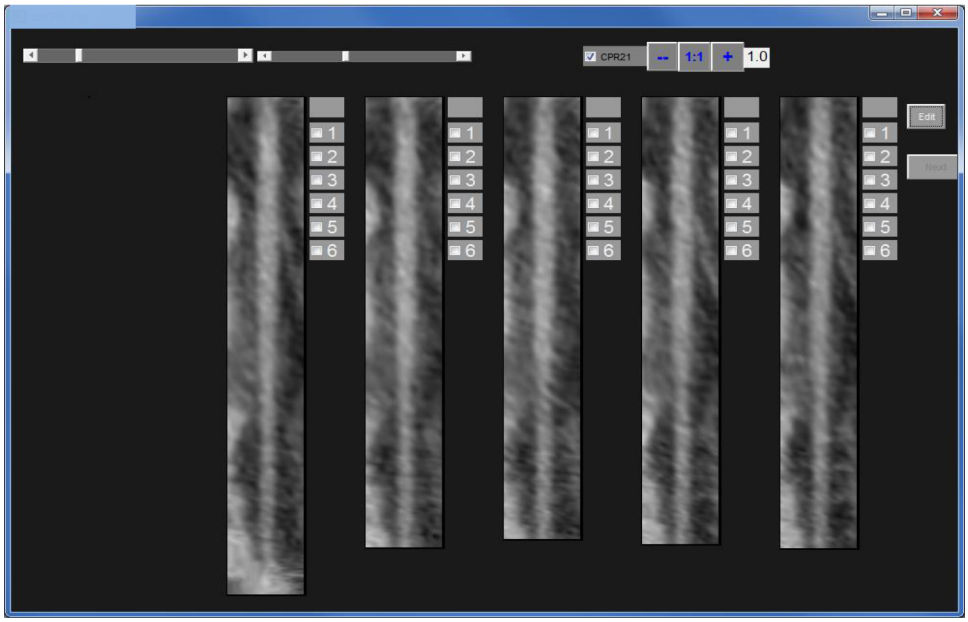

FIG. 4. An example for which only five corresponding segments were found in the six phases by the RCSM method because the corresponding vessel segment could not be extracted and tracked in one of the phases. The rankings of the vessel quality ranged from 1 to 6 with 1 being the best. The labels S_j ($j = 1, \ldots, 6$) are added to indicate the order of the images in the figure to facilitate the discussion in Table III; they were not displayed during the observer experiment.

107, respectively, while the percentages for the observers' top 2 selections were calculated relative to two times the total number of vessel segment groups in each tree because 2 vessels with rankings of 1 and 2 were counted for each group.

4. DISCUSSION

Automated segmentation and tracking the coronary arteries is a fundamental step to select the best-quality coronary arterial segment from different cCTA phases. Many factors, such as irregular heartbeats, incorrect contrast timing, narrowing and blockages caused by coronary plaques, and other noise artifacts can cause poor quality of a vessel and the failure of automated vessel segmentation and tracking. Both missing branches and false positives (FPs), such as coronary veins, in the tracked coronary arterial trees from different phases make it more challenging for automated registration of coronary trees in multiple phases. In addition, the average displacements of the left and right coronary trees in adjacent phases are different due to the physiological fact that the right coronary tree in general has greater motion than the left coronary tree. The performances of our methods for segmentation and tracking of the coronary arteries and for the registration of the left and right coronary trees in multiple phases have been described in detail previously.[17–19]

To identify the corresponding coronary segments, our RCSM method starts with the longest coronary branch among all branches in the available phases. The longest branch that is identified from the root of the coronary artery to the distal end usually contain more than one coronary segments; for example, the branch most often found to be the longest in the left coronary tree contains segments of left main, proximal left anterior descending (LAD), mid-LAD, and distal LAD arteries. The success of segmenting and tracking a long vessel to the distal end in one phase often indicates that the vessel has a better quality than those corresponding but shorter tracked vessels in the other phases. Using the longest tracked vessel branch as a starting point establishes a tree-stem landmark that can simplify the recursive procedure of the RCSM method in finding the corresponding vessel segments among a large number of vessel segments in multiple phases. The difference between the artery segments identified by our method and those by the AHA 17-segment model is not a problem because we envision that the selected segment being displayed for clinician's interpretation can be shown

TABLE I. Agreement between the automated method and human observers in identifying the best-quality coronary artery segments from multiple-phase cCTA.

Automated method	Radiologist	Observer 1	Observer 2	Observer 3	Observer 4
Agreement within top 1 ranking (%)	61.4	54.7	61.4	70.5	61.0
Agreement within top 2 rankings (%)	78.3	76.8	84.3	83.9	85.8
Agreement within top 3 rankings (%)	89.8	87.8	92.9	89.4	94.5

TABLE II. The agreement between the radiologist and the other four observers evaluated by the percentages of the 254 groups for which an observer's top ranked segment agreed with the radiologist's top 2 ranked segments, and the Cohen's kappa values and confidence intervals. The agreement between the AI-BQ segment and the radiologist's top 2 ranked segments is also shown for comparison.

	Observer 1	Observer 2	Observer 3	Observer 4	AI-BQ
Percentage agreement (%)	79.9	80.7	82.3	76.8	78.3
Kappa[a]	0.64 ± 0.05	0.65 ± 0.05	0.68 ± 0.05	0.56 ± 0.05	0.60 ± 0.05
95% confidence intervals of kappa	[0.54, 0.73]	[0.56, 0.74]	[0.59, 0.77]	[0.47, 0.67]	[0.50, 0.70]

[a]The following kappa values have been suggested to define interobserver agreement: poor (0), slight (0–0.20), fair (0.21–0.40), moderate (0.41–0.60), substantial (0.61–0.80), and excellent (0.81–0.99) (Ref. 21).

on a "roadmap" in a "navigation" window that highlights the corresponding segment(s) on the coronary tree. Alternatively, a coronary artery labeling algorithm may be developed to identify and display the selected segments following the 17-segment model.

The cyclic cardiac motion between systole and diastole causes the blurring of the coronary artery trees. Figure 5 shows that although the majority of the AI-BQ segments and the observers' top 2 rankings are identified from the 70% to 80% phases approximating end-diastole for the left and right coronary trees, an average of about 35% and 27% of AI-BQ segments and the observers' top 2 rankings for the left and right coronary trees, respectively, were identified from the 40% to 50% phases, which approximate end systole. This reveals that a substantial number of coronary arteries have better image quality in the lower phases. Automated selection of the individual best-quality arterial segments, instead of a single optimal cCTA phase as a whole, may better extract the most motion free and therefore the most accurate data representing the coronary arteries available from multiple-phase cCTA, and potentially improve the diagnostic accuracy for coronary arterial disease.

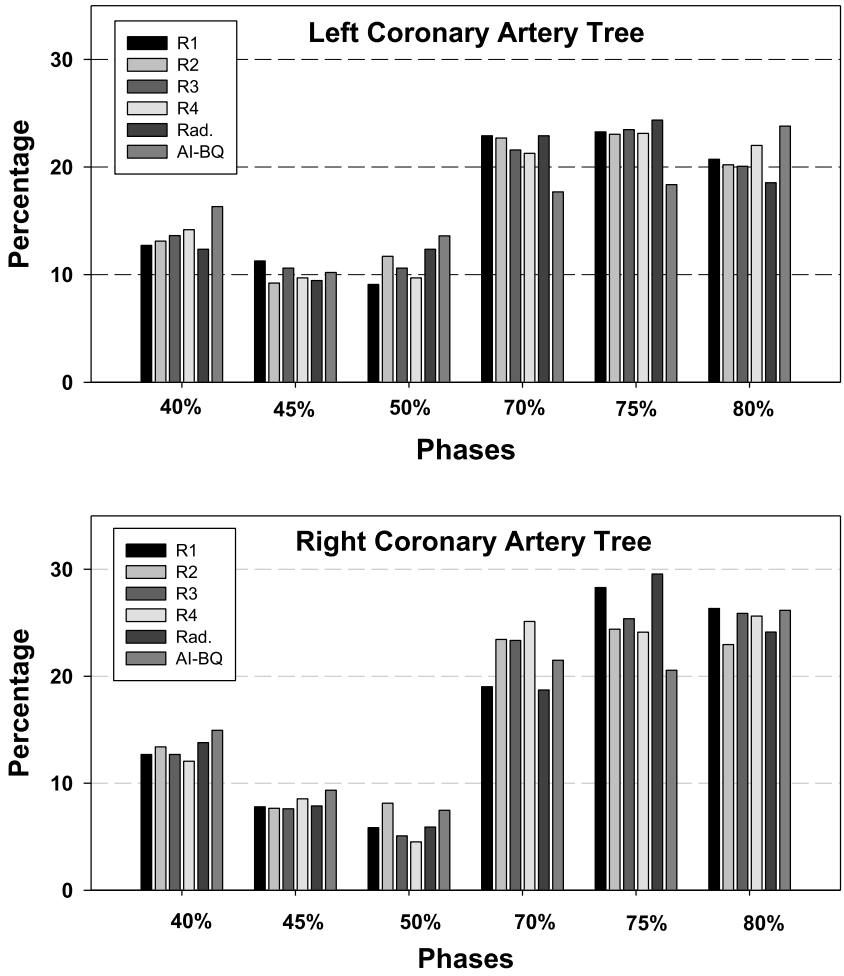

FIG. 5. The distributions of the percentages of the segments that were selected from the available phases and ranked as the top 2 by five observers in the six cCTA phases. The percentages of the automatically identified best-quality (AI-BQ) segments were also plotted for comparison. (Top) Left coronary artery tree. (Bottom) Right coronary artery tree. The percentages were calculated relative to the respective tree.

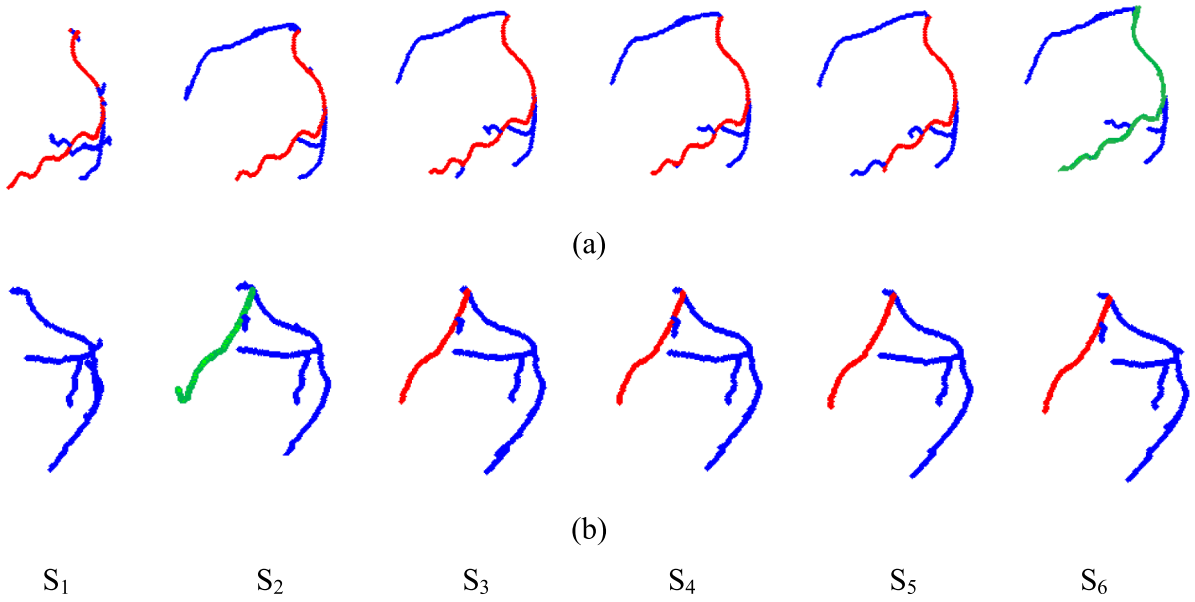

FIG. 6. The reference coronary segment (green) in a recursive cycle of RCSM and its matched segments (red) are displayed in the multiple-phase left coronary artery trees. The corresponding CPR images of the highlighted (green and red) vessel segments in (a) and (b) are shown in Figs. 3 and 4, respectively. In (b), the LAD segment is missing in S_1 because it could not be tracked and extracted in this tree. The labels S_j ($j = 1, \ldots, 6$) correspond to those in the respective figure and Table III. (See color online version.)

To evaluate the accuracy of the RCSM method, the automated matched corresponding vessel segments from the multiple cCTA phases are visually examined by an experienced medical imaging researcher. For this evaluation, the reference segment in a recursive cycle of RCSM and its matched segments are highlighted in green and red colors, respectively, on the vessel tree and displayed along with the GUI used for the observer preference study that showed the corresponding CPR segments; for example, Fig. 6(a) was displayed below Fig. 3, Fig. 6(b) was displayed below Fig. 4. The GUI allows the evaluator to rotate the coronary artery tree in three dimensions to examine the location of each matched segments and determine whether it was a corresponding vessel. In 203 of the 254 vessel groups containing 763 vessel segments, the corresponding vessels from different phases were found to be correctly identified by the RCSM method. In the remaining 51 groups that contain 228 corresponding segments, 65 segments were mistakenly identified as the corresponding segments. Of the 65 segments, 12, 14, 10, 10, and 18 segments were ranked among the top 2 by observer R_1, R_2, R_3, R_4 and the radiologist, respectively. However, none were identified as the best-quality segments by the automated method. Of 999 tracked vessel segments, 8 FP segments were segmented and tracked in one of 6 phases. Six of them were not identified as the AI-BQ segments by our automated method, indicating that utilizing the automated identification of best-quality coronary segments from different phases has the potential to reduce FPs in automated tracking of coronary artery trees because the FPs such as veins have less chance to be selected as the best quality vessels compared with true arteries.

Because there is no ground truth to measure which coronary segments are the best quality among corresponding segments in different phases. Our observer preference study was performed to provide a reference standard to evaluate the performance of the automated method for identification of best-quality segments. In this study, five observers including an experienced thoracic cardiac radiologist assessed the rankings of the vessel quality for corresponding segments in different phases. Table III shows the ranking of the vessel segments by the five observers for the examples in Figs. 3 and 4. Although the visual differences in the quality of the corresponding segments in each group of corresponding vessels are very small, for the vessel group in Fig. 3, one segment (S_2) was ranked among the top 2 by all five observers

TABLE III. The rankings of 1–6 (1 = best) by one experienced cardiothoracic radiologist and four experienced medical imaging researchers (R_1–R_4), and the AI-BQ segments in the two groups of corresponding vessel segments shown in Figs. 3 and 4. Note that the labels S_j ($j = 1, \ldots, 6$) are used to indicate the images displayed in the figures for one of the observers. The rankings of the same segment from different observers are arranged in the same row for comparison in this table although the images were displayed to each observer in a randomized order.

		Radiologist	R_1	R_2	R_3	R_4	AI-BQ
Figure 3	S_1	4	5	6	6	6	
	S_2	2	1	1	2	1	
	S_3	1	3	4	1	2	1
	S_4	3	2	2	4	4	
	S_5	6	4	5	5	5	
	S_6	5	6	3	3	3	
Figure 4	S_1						
	S_2	3	5	4	4	1	
	S_3	4	3	3	3	2	
	S_4	5	4	5	5	3	
	S_5	2	2	1	2	5	1
	S_6	1	1	2	1	4	

and another segment (S_3) was ranked among the top 2 by three observers and selected by the automated method; for the group shown in Fig. 4, four observers ranked the same two segments (S_5, S_6) to be the top 2 and one of which (S_5) was the AI-BQ segment. For the 254 vessel groups, the agreement between the top 2 rankings of the radiologist and the best-quality vessel by the automated method was 78.3% (Table I). The agreement between the radiologist's top 2 ranking and the top rankings of the other four observers averaged 79.9% ± 2.3% (range: 76.8%–82.3%) (Table II). These results indicate that the performance of the automated method for the identification of the AI-BQ vessel is comparable to that of the human observers selecting the top ranked vessels. In addition, 89.4% of AI-BQ segments agreed with at least two observers' top 2 rankings, and 96.5% agreed with at least one observer's top 2 rankings. This demonstrates the feasibility of using our automated method to identify the best quality segments among different phases.

In comparison with our previous pilot study[16] that demonstrated the feasibility of an automated best-quality vessel segment identification approach using a single feature and two cCTA cases, our current approach uses a new method to improve the matching of corresponding segments from different phases, extracts new features from the original CT volume in addition to the straightened CPR vessel volume, and identifies the best-quality segments by using a newly designed weighted voting ensemble classifier. The observer preference study with five observers confirms that the automated method has reasonable performance, within the variability of human observers, in selecting best-quality vessels from multiple-phase cCTA. Although the results show the promise of this approach, one limitation is the relatively small number of cases. A larger training data set will allow designing more complex classifiers and/or additional image features to characterize the quality of the vessels, which may further improve the performance of the automated method.[24,25] *A large test data set is also needed to include the variety of relevant clinical occurrences of coronary abnormalities in cCTA (e.g., different types of plaques of different degrees of occlusions at different segments of the coronary trees), so that the robustness of the method can be assessed in cases more representative of the patient population*. Another limitation is that the current method is not fully automated, requiring a manually marked seed point at the origin of each coronary artery tree to initiate the tracking of the tree. This step will be replaced when we can develop a reliable method to identify the seed point location accurately and automatically. *Besides the manual identification of the seed points, the other processes are all automatically performed without any user interaction in this study*. Ultimately, after the automated method for best-quality vessel selection is fully developed and its robustness validated, the usefulness of this method for improving the detection of atherosclerotic plaques in cCTA by radiologists or a computer-aided detection system, *as well as its potential benefits in improving workflow and consistency in the selection of the coronary arteries for interpretation*, will need to be investigated in future studies.

5. CONCLUSION

We developed an automated method for the matching of corresponding segments from coronary artery trees extracted from multiple phases of a cCTA examination, and designed a new weighted voting ensemble classifier using four vessel quality measures for identification of the best-quality segment among the corresponding segments. The results of our observer preference study showed that the performance of the automated method was comparable, within the interobserver variations, to the selection of the best-quality coronary segments from the multiple cCTA phases by human observers. The study demonstrates the potential of using our automated method to identify the best-quality phase for individual coronary arteries. The virtual composite coronary artery trees containing the collection of the best-quality coronary segments selected from all phases will enable interpreting physicians to fully utilize the best available information in cCTA for diagnosis of coronary disease, without requiring manual search through the multiple phases and minimizing the variability in image phase selection for evaluation of coronary artery segments across the diversity of human readers with variations in expertise. The automated method will also be useful as a preprocessing step in a computer-aided image analysis system for detection of atherosclerotic plaques in cCTA.

ACKNOWLEDGMENT

This work is supported by National Institutes of Health Grant No. R01 HL106545.

CONFLICT OF INTEREST DISCLOSURE

The authors have no COI to report.

[a]Author to whom correspondence should be addressed. Electronic mail: chuan@umich.edu

[1]M. J. Budoff, S. Achenbach, R. S. Blumenthal, J. J. Carr, J. G. Goldin, P. Greenland, A. D. Guerci, J. A. C. Lima, D. J. Rader, G. D. Rubin, L. J. Shaw, and S. E. Wiegers, "Assessment of coronary artery disease by cardiac computed tomography: A scientific statement from the American Heart Association Committee on Cardiovascular Imaging and Intervention, Council on Cardiovascular Radiology and Intervention, and Committee on Cardiac Imaging, Council on Clinical Cardiology," Circulation **114**, 1761–1791 (2006).

[2]Writing group Members, D. Lloyd-Jones, R. Adams, M. Carnethon, G. De Simone, T. B. Ferguson, K. Flegal, E. Ford, K. Furie, A. Go, K. Greenlund, N. Haase, S. Hailpern, M. Ho, V. Howard, B. Kissela, S. Kittner, D. Lackland, L. Lisabeth, A. Marelli, M. McDermott, J. Meigs, D. Mozaffarian, G. Nichol, C. O'Donnell, V. Roger, W. Rosamond, R. Sacco, P. Sorlie, R. Stafford, J. Steinberger, T. Thom, S. Wasserthiel-Smoller, N. Wong, J. Wylie-Rosett, and Y. Hong, "Heart disease and stroke statistics–2009 update: A report from the American Heart Association Statistics Committee and Stroke Statistics Subcommittee," Circulation **119**, e21–181 (2009).

[3]J. J. Fine, C. B. Hopkins, N. Ruff, and F. C. Newton, "Comparison of accuracy of 64-slice cardiovascular computed tomography with coronary angiography in patients with suspected coronary artery disease," Am. J. Cardiol. **97**, 173–174 (2006).

[4]M. Budoff, D. Dowe, J. Jollis, M. Gitter, J. Sutherland, E. Halamert, M. Scherer, R. Bellinger, A. Martin, R. Benton, A. Delago, and J. Min, "Diagnostic performance of 64-multidetector row coronary computed tomographic angiography for evaluation of coronary artery stenosis in individuals without known coronary artery disease: Results from the prospective

multicenter accuracy (assessment by coronary computed tomographic angiography of individuals undergoing invasive coronary angiography) trial," J. Am. Coll. Cardiol. **52**, 1724–1732 (2008).
[5]J. Min, L. Shaw, R. Devereux, P. Okin, J. Weinsaft, D. Russo, N. Lippolis, D. Berman, and T. Callister, "Prognostic value of multidetector coronary computed tomographic angiography for prediction of all-cause mortality," J. Am. Coll. Cardiol. **50**, 1161–1170 (2007).
[6]M. Garcia, J. Lessick, M. Hoffmann, and C. S. Investigators, "Accuracy of 16-row multidetector computed tomography for the assessment of coronary artery stenosis," JAMA **296**, 403–411 (2006).
[7]B. Desjardins and E. A. Kazerooni, "ECG-gated cardiac CT," Am. J. Roentgenol. **182**, 993–1010 (2004).
[8]J. Wei, C. Zhou, H.-P. Chan, A. Chughtai, S. Patel, P. Agarwal, J. Kuriakose, L. M. Hadjiiski, and E. Kazerooni, "Computerized detection of non-calcified plaques in coronary CT angiography: Evaluation of topological soft gradient prescreening method and luminal analysis," Med. Phys. **41**, 081901 (9pp.) (2014).
[9]V. Rasche, B. Movassaghi, M. Grass, D. Schafer, and A. Buecker, "Automatic selection of the optimal cardiac phase for gated three-dimensional coronary x-ray angiography," Acad. Radiol. **13**, 630–640 (2006).
[10]M. H. K. Hoffmann, J. Lessick, R. Manzke, F. T. Schmid, E. Gershin, D. T. Boll, S. Rispler, A. J. Aschoff, and M. Grass, "Automatic determination of minimal cardiac motion phases for computed tomography imaging: Initial experience," Eur. Radiol. **16**, 365–373 (2006).
[11]R. M. S. Joemai, J. Geleijns, W. J. H. Veldkamp, and L. J. M. Kroft, "Clinical evaluation of 64-slice CT assessment of global left ventricular function using automated cardiac phase selection," Circ. J. **72**, 641–646 (2008).
[12]R. M. S. Joemai, J. Geleijns, W. J. H. Veldkamp, A. de Roos, and L. J. M. Kroft, "Automated cardiac phase selection with 64-MDCT coronary angiography," Am. J. Roentgenol. **191**, 1690–1697 (2008).
[13]B. Ruzsics, M. Gebregziabher, H. Lee, R. L. Brothers, T. Allmendinger, S. Vogt, P. Costello, and U. J. Schoepf, "Coronary CT angiography: Automatic cardiac-phase selection for image reconstruction," Eur. Radiol. **19**, 1906–1913 (2009).
[14]C. Rohkohl, H. Bruder, K. Stierstorfer, and T. Flohr, "Improving best-phase image quality in cardiac CT by motion correction with MAM optimization," Med. Phys. **40**, 031901 (15pp.) (2013).
[15]W. G. Austen, J. E. Edwards, R. L. Frye, G. G. Gensini, V. L. Gott, L. S. Griffith, D. C. McGoon, M. L. Murphy, and B. B. Roe, "A reporting system on patients evaluated for coronary artery disease. Report of the Ad Hoc Committee for Grading of Coronary Artery Disease, Council on Cardiovascular Surgery, American Heart Association," Circulation **51**, 5–40 (1975).
[16]J. Liu, L. Hadjiiski, H.-P. Chan, C. Zhou, J. Wei, A. Chughtai, J. Kuriakose, P. Agarwal, and E. Kazerooni, "Automatic selection of best quality vessels from multiple-phase coronary CT angiography (cCTA)," Proc. SPIE **9414**, 94140E1–94140E9 (2015).
[17]C. Zhou, H.-P. Chan, A. Chughtai, S. Patel, L. M. Hadjiiski, J. Wei, and E. A. Kazerooni, "Automated coronary artery tree extraction in coronary CT angiography using a multiscale enhancement and dynamic balloon tracking (MSCAR-DBT) method," Comput. Med. Imaging Graphics **36**, 1–10 (2012).
[18]C. Zhou, H.-P. Chan, A. Chughtai, J. Kuriakose, P. Agarwal, E. A. Kazerooni, L. M. Hadjiiski, S. Patel, and J. Wei, "Computerized analysis of coronary artery disease: Performance evaluation of segmentation and tracking of coronary arteries in CT angiograms (CTA)," Med. Phys. **41**, 081912 (11pp.) (2014).
[19]L. Hadjiiski, C. Zhou, H.-P. Chan, A. Chughtai, P. Agarwal, J. Kuriakose, E. Kazerooni, J. Wei, and S. Patel, "Coronary CT angiography (cCTA): Automated registration of coronary arterial trees from multiple phases," Phys. Med. Biol. **59**, 4661–4680 (2014).
[20]C. Zhou, H.-P. Chan, J. W. Kuriakose, A. Chughtai, J. Wei, L. M. Hadjiiski, Y. Guo, S. Patel, and E. A. Kazerooni, "Pulmonary vessel segmentation utilizing curved planar reformation and optimal path finding (CROP) in computed tomographic pulmonary angiography (CTPA) for CAD applications," Proc. SPIE **8315**, 83150N1–83150N9 (2012).
[21]M. S. Kramer and A. R. Feinstein, "Clinical biostatistics: LIV. The biostatistics of concordance," Clin. Pharmacol. Ther. **29**, 111–123 (1981).
[22]C. Zhou, H.-P. Chan, B. Sahiner, L. M. Hadjiiski, A. Chughtai, S. Patel, J. Wei, J. Ge, P. N. Cascade, and E. A. Kazerooni, "Automatic multiscale enhancement and hierarchical segmentation of pulmonary vessels in CT pulmonary angiography (CTPA) images for CAD applications," Med. Phys. **34**, 4567–4577 (2007).
[23]S. Achenbach, W. Moshage, D. Ropers, and K. Bachmann, "Curved multiplanar reconstructions for the evaluation of contrast-enhanced electron-beam CT of the coronary arteries," Am. J. Roentgenol. **170**, 895–899 (1998).
[24]B. Sahiner, H.-P. Chan, N. Petrick, R. F. Wagner, and L. M. Hadjiiski, "Feature selection and classifier performance in computer-aided diagnosis: The effect of finite sample size," Med. Phys. **27**, 1509–1522 (2000).
[25]H.-P. Chan, B. Sahiner, R. F. Wagner, and N. Petrick, "Classifier design for computer-aided diagnosis: Effects of finite sample size on the mean performance of classical and neural network classifiers," Med. Phys. **26**, 2654–2668 (1999).